# Quartz Thermoluminescence Spectra in the High-Dose Range

Christoph Schmidt[1,*], Clemens Woda[2]

[1] Chair of Geomorphology & BayCEER, University of Bayreuth, 95440 Bayreuth, Germany
[2] Helmholtz-Zentrum München, German Research Centre for Environmental Health, Institute of Radiation Medicine, Ingolstädter Landstraße 1, 85764 Neuherberg, Germany
* Corresponding author: christoph.schmidt@uni-bayreuth.de, Tel.: +49-921-552267

## Abstract

The red thermoluminescence (RTL) emission of quartz is associated with advantageous features such as high saturation dose and good reproducibility. Previous studies, however, noted inexplicable RTL glow curve shapes with new peaks at large doses (kGy range). Here we present TL spectra of two granitic quartz samples over the additive γ-dose range 0.1–47.9 kGy. While for doses between 0.4 and 1 kGy the TL spectra are dominated by the red emission at 1.95 eV (630 nm), a blue emission at 2.67 eV (465 nm) becomes prominent for higher doses. For one sample, this blue component completely dominates the spectrum for doses >12.2 kGy with intensity maxima around 200 °C and >350 °C (heating rate 2 K $s^{-1}$). The other sample still contains well resolvable red and blue emissions at the largest dose with similar TL peak positions. Signal saturation for the blue emission in the glow curve range 260–300 °C is not yet reached following an additive γ-dose of 47.9 kGy, whereas the red emission generally shows a more subdued signal response for doses >5–12 kGy. These findings agree qualitatively with additional monochromatic blue and red TL measurements on the same samples. The evolution of supplementary radiofluorescence spectra over the entire γ-dose range is more complex, but suggests that the sensitisation of the blue wavelength region occurs during heating and not during irradiation and through creation of electron traps rather than recombination centres (most likely $[AlO_4]^0$ sites). The sharp sensitivity increase at 1 kGy might likewise be related to alkali ion redistribution and/or the removal of non-radiative competitive recombination pathways. While the blue emission still requires thorough investigation, care should be taken when recording RTL using optical filters since significant portions of the registered TL could originate from the blue component entering the RTL transmission window. In practical terms, the dose-dependent change in relative intensities of blue and red TL emissions might help in detecting exposure to high doses.

Keywords: Luminescence; Radiofluorescence; Red thermoluminescence; Gamma-dose; Sensitivity change; Recombination centre

## Introduction

The thermally stimulated luminescence (TL) signal of natural quartz has been extensively used for retrospective dosimetry and dating of geological and archaeological materials during the past decades (see, e.g., Aitken 1985 or Wintle 2008 for an overview of applications). The TL emission spectrum of quartz usually comprises three main bands centred on ~380 nm (3.3 eV), ~470 nm (2.6 eV) and ~620 nm (2.0 eV), while for quartz types of distinct formation conditions additional emissions have been reported, e.g. a band at 420–435 nm in igneous quartz or one at 560–580 nm in hydrothermal vein quartz (Rink et al. 1993; Scholefield et al. 1994; Itoh et al. 2002).

In TL dating, usually the UV (360–380 nm) band is measured as monochromatic glow curve by means of optical filters to estimate the absorbed dose. Compared to the UV emission, the red TL (RTL) emission at around 620 nm is more difficult to measure due to interference with blackbody radiation at temperatures >300 °C, but RTL was attributed remarkable advantageous properties. Firstly, the RTL saturation dose level was observed to be of the order of several hundred or even several thousand Gy (Pilleyre et al. 1992; Fattahi and Stokes 2000; Ganzawa and Maeda 2009; Richter et al. 2017) and hence substantially higher than that of the UV emission (Murray and Wintle 2000; Jain et al. 2007). RTL would thus allow extending the dating range to 1 Ma or even beyond under favourable conditions. Secondly, the RTL sensitivity was reported to change only slightly or even insignificantly with irradiation and thermal treatments, making it attractive for single-aliquot regeneration procedures to estimate the absorbed dose (Richter and Krbetschek 2006; Zöller et al. 2014; Richter et al. 2017).

Due to its unique luminescence properties, the RTL emission of quartz was recently suggested by Schmidt et al. (2015) for use in thermochronometry. Unlike non-saturating thermochronometric systems (e.g., the noble gas systems (U-Th)/He or $^{40}Ar/^{39}Ar$; Reiners and Brandon 2006), the luminescence signal of minerals approaches a level of dose saturation beyond which temporal information cannot be resolved anymore. Consequently, dose rates in the range 3–6 Gy $ka^{-1}$ allow cooling histories to be reconstructed only for the past 100–200 ka for most quartz and feldspar signals, which makes this method valuable merely for rapidly exhuming Alpine orogens (cf. King et al. 2016a,b). Based on reported values of characteristic saturation dose of RTL from quartz, this signal could be used to extended that period by about one order of magnitude. However, in this previous study on exploring the potential of RTL for this purpose, additive RTL glow curves from granitic quartz extracted from a borehole showed a shift of peak positions and/or the emergence of a new peak for additive β-doses >2 kGy with the consequence of failed heating plateau tests (Fig. 4 in Schmidt et al. 2015). This observation can be explained either with non-first-order behaviour of TL peaks or with a shift of TL emission bands as a function of dose (Rink et al. 1993; Scholefield and Prescott 1999). Similarly, RTL glow curves recorded by Montret et al. (1992) and Fattahi and Stokes (2000) demonstrated shift in TL peak position with dose, and Pilleyre et al. (1992) and Miallier et al. (1994) reported large differences in intensity and shape of the first- and second-glow RTL dose response curves of heated natural quartz grains at large doses (<16 kGy), which impeded reliable regression to obtain the palaeodose.

Potential interference of RTL with other emissions can be best studied by means of TL spectrometry (Townsend 1994). Most of previously published quartz TL spectra were recorded following doses <500 Gy; only few studies employed doses in the kGy-range (Hashimoto et al. 1987, 1993; Huntley et al. 1988a,b; Kuhn et al. 2000; Woda et al. 2002; Westaway and Prescott 2012; Guzzo et al. 2017; Hunter et al. 2018). In essence, it was found that the relative proportions of the blue (~470 nm) and red (~620 nm) TL emissions may change as a function of large doses, albeit the effect appears to be strongly sample-dependent.

In view of these previous findings, the present study seeks to identify the dose response behaviour and interference of individual quartz TL emissions in the high-dose range. Our experiments are intended to clarify to which extent monochromatic TL measurements of quartz really capture individual emissions or rather represent a mixture of signals from luminescence centres with different physical properties. We therefore use additive doses up to 47.9 kGy to explore the entire dose range up to expected saturation

of the RTL signal. The dataset is completed by monochromatic blue and red TL measurements following additive β- and γ-irradiation of a set of quartz samples, since for additive doses below 1 kGy, the signal intensity was too low for spectral measurements in some cases. The results, which unveil the cause of the peak shift in the RTL glow curves shown in Schmidt et al. (2015), are discussed regarding their implications for dating and thermochronometry.

## Material and methods

### *Samples, sample preparation and irradiation*

One sample for spectrometric analyses in this study originates from a geothermal borehole (wash boring) in Late Variscan granitic bedrock near Weißenstadt in the Fichtelgebirge, Germany (laboratory code BT1229, 1364 m depth below surface, ambient temperature of 39 °C). The second sample represent a consolidated sample from the same lithological unit (laboratory code BT1284, 2 m depth below surface, ambient temperature of 5 °C). These two samples were chosen for spectral measurements since for these additive RTL dose response curves have been constructed in the precursor study (Schmidt et al. 2015). The extraction of pure quartz grains in the size range 90–200 µm from the consolidated rock sample (BT1284) and the bore cuttings (BT1229) is described in detail in Schmidt et al. (2015). Samples were not exposed to daylight or thermally treated prior to spectral or monochromatic TL analyses.

To examine the dose response and signal stability of individual emissions by means of monochromatic TL measurements for additional varieties of natural quartz, three further sand-sized (90–200 µm) quartz samples with natural doses expected to exceed 1 kGy were studied: The consolidated rock sample BT1647 was extracted from the same lithological unit as samples BT1229 and BT1284 (Weißenstadt granite) from a depth of 2 m below surface and served as a reference sample with respect to the spectrometry results (due to scarcity of sample material of BT1229 and BT1284). Due to the palaeozoic origin of the granite and the comparatively high dose rate in this type of rock (see Schmidt et al. 2015), it is reasonable to assume the natural TL signal of BT1647 to be in field saturation. Sample BT1629 represents a quartzitic sandstone from the Pre-Cambrian Roraima Group forming the tepui in the Gran Sabana of Venezuela (taken near the village of Canaima), which has an estimated minimum age of 1.5–1.6 Ga (Briceño and Schubert 1990; Briceño et al. 1990). Clastic grains within the quartzite are dominated by quartz (~95–98%), with minor contribution of feldspar, mica and heavy minerals (Chalcraft and Pye 1984; Doerr 1999). The natural dose is thus expected to be in the range of several hundred kGy. Quartz purification for these two samples followed the same routines as described in Schmidt et al. (2015). Sample BT1385 originates from deposits within the Druze marshland near Azraq, Jordan, see Ames et al. (2014) or Ames and Cordova (2015) for general information on the setting. Pure quartz was prepared as described in detail in Kolb et al. (2016). Infrared stimulated luminescence measurements of the K-rich feldspar fraction (90–200 µm) of this sample yielded a natural dose of ~1 kGy (not corrected for anomalous fading); the optically stimulated luminescence signal of quartz (detected in the UV emission range) was in dose saturation (unpublished data).

Each of the samples BT1284 and BT1229 was split into six subsamples, which were irradiated with an additive γ-dose of 0.1, 0.4, 1, 4, 12.2 and 47.9 kGy. The γ-doses were delivered by a $^{60}$Co-source "Gammacell 220", with a closed irradiation chamber of 0.152 m diameter and 0.206 m height and a dose-rate at the time of irradiations of 7.8 Gy min$^{-1}$. From each subsample three aliquots were prepared for TL spectrometry.

### *Thermoluminescence spectrometry*

Spectral measurements in the wavelength range of 300 nm to approx. 800 nm were done using a Freiberg Instruments lexsyg research system (Richter et al. 2013), equipped with an emission spectrometry unit,

consisting of a TE cooled Andor Technology iDus 420 Series CCD camera and a Shamrock 163 spectrometer. TL spectra were recorded with a heating rate of 2 K $s^{-1}$ and an integration time of 20 s up to a maximum temperature of 380 °C.

Before measurement of the TL spectra, radiofluorescence (RF) spectra were acquired during irradiation with the built-in $^{90}Sr/^{90}Y$ source of the reader (dose rate of ~0.02 Gy $s^{-1}$) for 120 s, with an integration time of 40 s. Longer integration times were not practical, as the number of interfering peaks due to cosmic rays can then become too large and peaks can partially overlap, which complicates an effective cleaning procedure. The RF signal was transmitted through a glass lens, cutting off any emission below 330 nm. The total imparted dose during RF measurement was 2.4 Gy, which is negligible compared to the previously administered γ-dose. All spectral measurements were first cleaned of peaks due to cosmic rays, background corrected and then corrected for the spectral response of the system, i.e. the combined, wavelength-dependent efficiency of the different components of the spectrometer (optical glass fiber, grating, camera), using a Bentham Instruments Ltd. calibration irradiance standard lamp (Type: CL 6). In case of the RF measurements, the three consecutive spectra obtained per sample were added to a single spectrum, in order to increase the signal-to-noise ratio.

Three-dimensional and contour plots were produced with the middle of the respective temperature interval being the reference temperature (e.g., the reference temperature of the interval 300–340 °C is 320 °C). For construction of a dose-response curve, Gaussian-shaped peak functions were fitted to the emission spectra. The TL spectrum of the aliquot having received the highest dose can be fitted with reasonable accuracy up to the highest temperature interval measured (340–380 °C). By contrast, the interval 260–300 °C was the highest temperature interval, where emission bands largely free of interference effects could be extracted from the spectra across the entire dose range. In this interval, thermal radiation was negligible for wavelengths below 500 nm, but could be reasonably well approximated by a Gaussian function for higher wavelengths (>600 nm). From repeated spectral measurements on (highly reproducible) $Al_2O_3$:C chips, the reproducibility of the measurements was assessed to be better than 2%. Inter-aliquot scatter for the quartz samples was <5% for stronger emissions (peak count rate (uncorrected) of 150–700 counts per channel) and 10-25% for weak emissions (peak count rate of 10–60 counts per channel, readout noise at 1.3 counts per channel), which is influenced by the uncertainty in the curve fitting analysis.

*Monochromatic thermoluminescence measurements*

Because the sensitivity of the spectrometric system was too low to evaluate the blue TL signal of sample BT1229 induced by γ-doses <1 kGy and because the temperature resolution of the spectral measurements was generally only 40 °C, we additionally conducted monochromatic TL measurements to capture the dose-response for specific emissions in this dose range and to better evaluate possible changes in the glow peak structure. TL glow curves were recorded with a Freiberg Instruments lexsyg research luminescence reader (Richter et al. 2013) equipped with a built-in $^{90}Sr/^{90}Y$ β-source (dose rate ~0.06 Gy $s^{-1}$; Richter et al. 2012). Blue TL (BTL) emissions were recorded with a Semrock BrightLine HC475/50 bandpass filter in front of a Hamamatsu H7360-02 bi-alkaline photomultiplier tube (PMT), while for RTL signals a Chroma ET 620/60x bandpass filter in combination with a thermo-electrically cooled Hamamatsu H7421-40 GaAsP PMT was used. With a spectral response of 300–720 nm, the latter is particularly suited for measuring the red emission centred on ~620 nm. Quantum efficiencies of the two PMTs and the transmission characteristics of the bandpass filters are shown in Fig. 1.

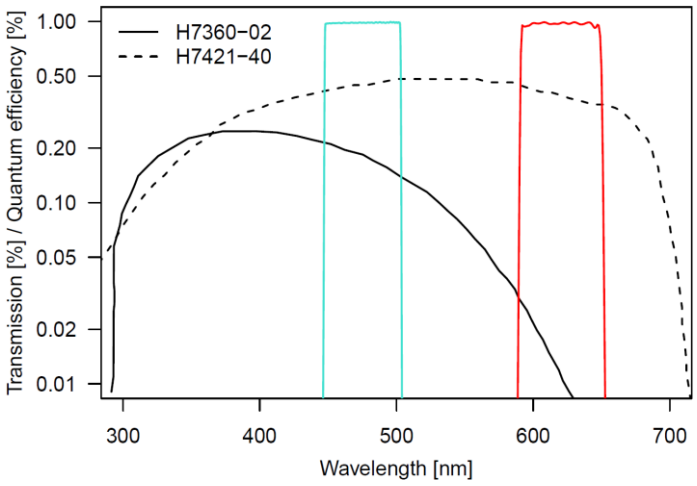


**Fig. 1** Quantum efficiency of the bi-alkaline Hamamatsu H7360-02 and the thermo-electrically cooled H7421-40 GaAsP photomultiplier tubes (PMT) and transmission spectra of the Semrock BrightLine HC475/50 (blue line) and Chroma ET 620/60x (red line) bandpass filters used for detection of monochromatic blue TL (BTL) and red TL (RTL), respectively.

All TL glow curves were recorded with a heating rate of 1 K $s^{-1}$ up to temperatures of 450 °C (BTL) and 430 °C (RTL). A second TL run with the same parameters after readout of the initial signal served to estimate the background signal resulting from instrumental noise and incandescence. This signal was subtracted to obtain the net signal. After depletion of the signal resulting from additive β- or γ-irradiation, BTL and RTL induced by a regenerative β-dose of 30 or 50 Gy was measured to monitor the sensitivity of samples following additive irradiation.

## Results

### *Thermoluminescence spectra following additive γ-irradiation*

For additive γ-doses ≤1 kGy (BT1229) and <0.4 kGy (BT1284), the TL spectra are dominated by a red emission which shows peaks at temperatures of ~200 °C, with the indication of a high-temperature RTL peak beyond 300 °C (Figs. 2 and 3). A minute BTL emission at ~200 °C becomes visible in the spectrum for additive doses of 0.4 kGy (BT1284) and 1 kGy (BT1129). By increasing the dose, the relative contribution of both emissions is shifted from red to blue, until the RTL emission at 200 °C is completely masked by the broadened BTL emission for doses of 47.9 kGy (BT1229) and 12.2 kGy (BT1284). In the higher temperature region, the situation is somewhat different for both samples. For sample BT1284, only the blue emission is visible (or present), with a shift in the peak temperature from ~325 °C (12.2 kGy) to >360 °C (47.9 kGy, outside the recorded temperature range) and with an intensity that eventually surpasses the 200 °C BTL emission for the largest measured dose. In contrast, for sample BT1229, the blue and red emission remain distinct features, also for the highest dose but again with peak temperatures >360°C. Furthermore, the emission at ~200 °C remains the most intense signal <350 °C and for doses up to 47.9 kGy. Low-temperature peaks are not contained in the spectra due to the storage time of 10 days between γ-irradiation and measurement. The results of the TL spectral measurements are in qualitative agreement with the results shown in Hunter et al. (2018), where a dominating blue emission for quartz from a sand deposit was also observed for doses ≥1 kGy.

The UV emission (360 nm) was generally not observed in our samples, except for sample BT1284 at doses ≤1 kGy, where it is visible as a minor feature in the TL spectra for the 180–220 °C and 260–300 °C temperature intervals, and possibly in the spectra of the lower temperature peak of the other sample.

For the low temperature peak, however, the signal-to-noise-ratio was too low for a successful consideration of the UV emission in the fitting approach (Fig. 4d).

210

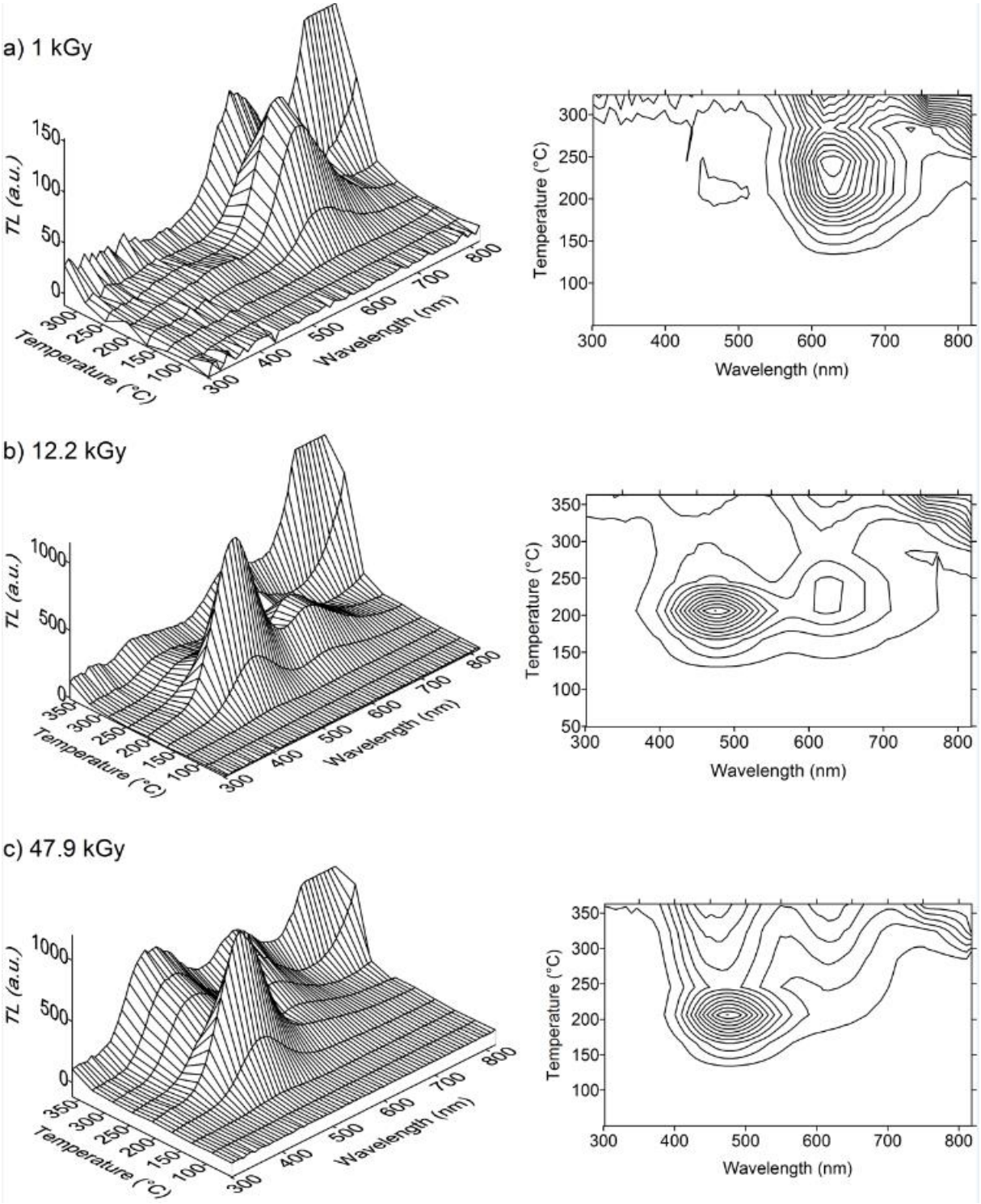


**Fig. 2** TL spectra of sample BT1229 for additive γ-doses of 1, 12.2 and 47.9 kGy, shown as 3D plots (left) and contour plots (right). Please see the main text for further details.

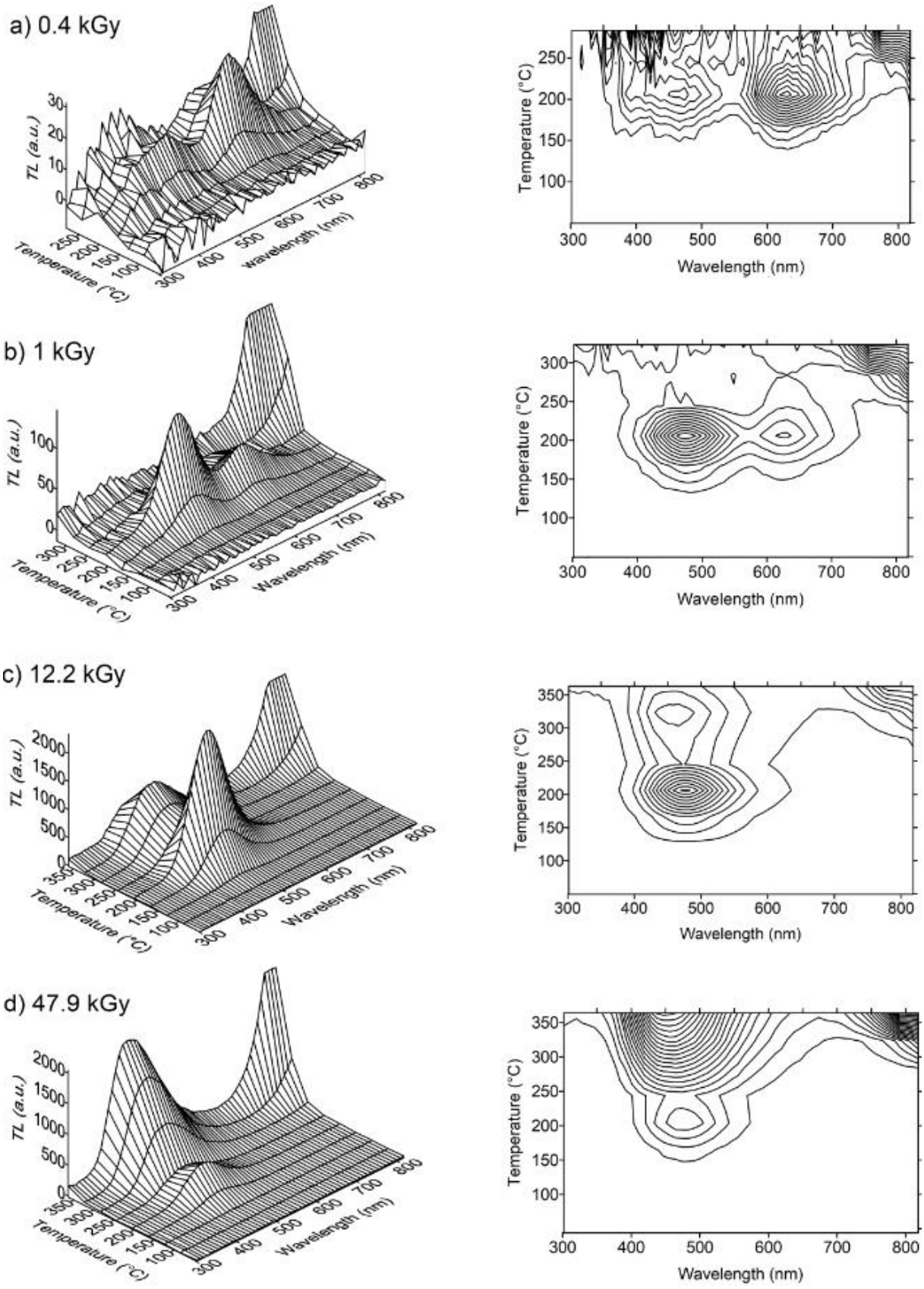


**Fig. 3** TL spectra of sample BT1284 for additive γ-doses of 0.4, 1, 12.2 and 47.9 kGy, shown as 3D plots (left) and contour plots (right). Please see the main text for further details.

220 Fitting individual Gaussian components to integrated spectra (intensity vs. energy) of 40 °C temperature intervals between 180 °C and 340 °C indicates that all spectra can be described by mainly two emissions at 2.67 eV (~465 nm) and 1.95 eV (630 nm) and that these emissions are involved in producing both the low and the high temperature TL peaks. This is shown in Fig. 4 for the integration intervals 180–220 °C and 260–300 °C and additive γ-doses of 1 kGy and 47.9 kGy.

225

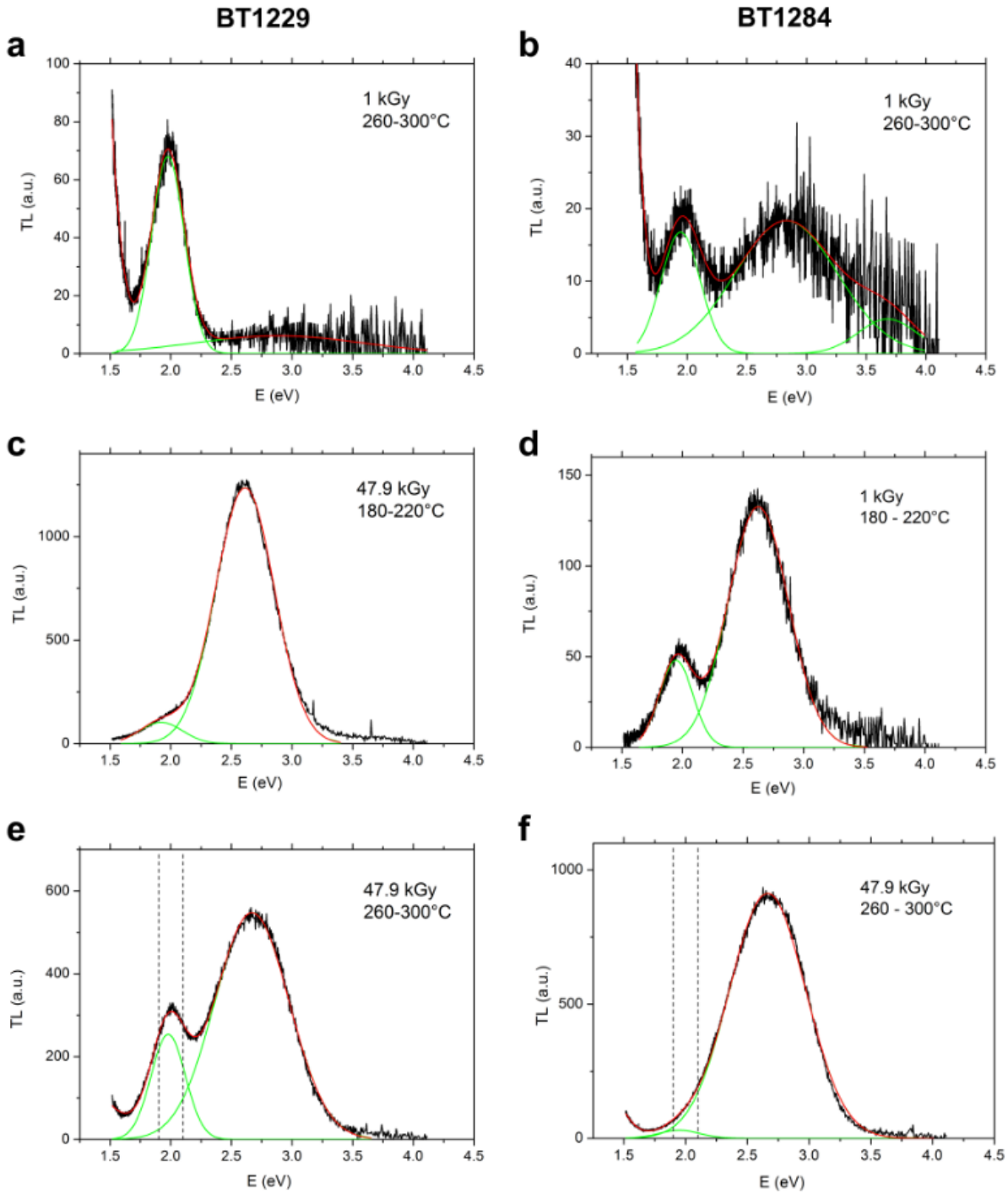


**Fig. 4** Integrated TL spectra (intensity vs. energy) of 40 °C temperature intervals between 180 °C and 300 °C for samples BT1229 (a, c, e) and BT1284 (b, d, f). These spectra were fitted with two to three individual Gaussian components, from which energies of 1.95 eV (630 nm) and 2.67 eV (465 nm) of the two main emissions were
230 extracted. Administered γ-doses as well as integration range are as indicated in the individual subplots. The dashed lines in subplots (e) and (f) visualise the transmission window for monochromatic red TL measurements.

Fig. 5 provides a graphical overview of the emission width (FWHM, in eV) and amplitude obtained from fitting of the TL spectra. Without constraining the fitting parameters, the energies of both emissions remain constant for both samples over the entire investigated dose range. A somewhat larger energy of the blue emission of ~2.9 eV at 1 kGy dose for sample BT1229 might be related to low signal intensity and problems in accurate fitting (see Fig. 4a). The emission width (FWHM, in eV) remains largely constant for both samples and emissions across the covered dose range, except for the blue component of sample BT1229, decreasing in width from ~1.6 eV at 1 kGy dose to 0.7 eV for >10 kGy (Fig. 5a,b). Fig 4. also serves to illustrate the level of interference one can expect in the red detection window by the blue emission in a PMT measurement. If the limits of the transmission window of the Chroma ET 620/60x bandpass filter are used as integration limits for the two emissions, then, for the highest dose applied and for sample BT1229, the red emission would contribute ~80% to a measured PMT signal with red filter and the blue emission about ~20%. In contrast, for BT1284 the red emission would only contribute ~20%, whereas the blue emission would contribute ~80% for the same detection window (Fig. 4e,f). This is a simplified calculation that does not take into account the efficiency of the PMT or the exact shape of the filter transmission curve.

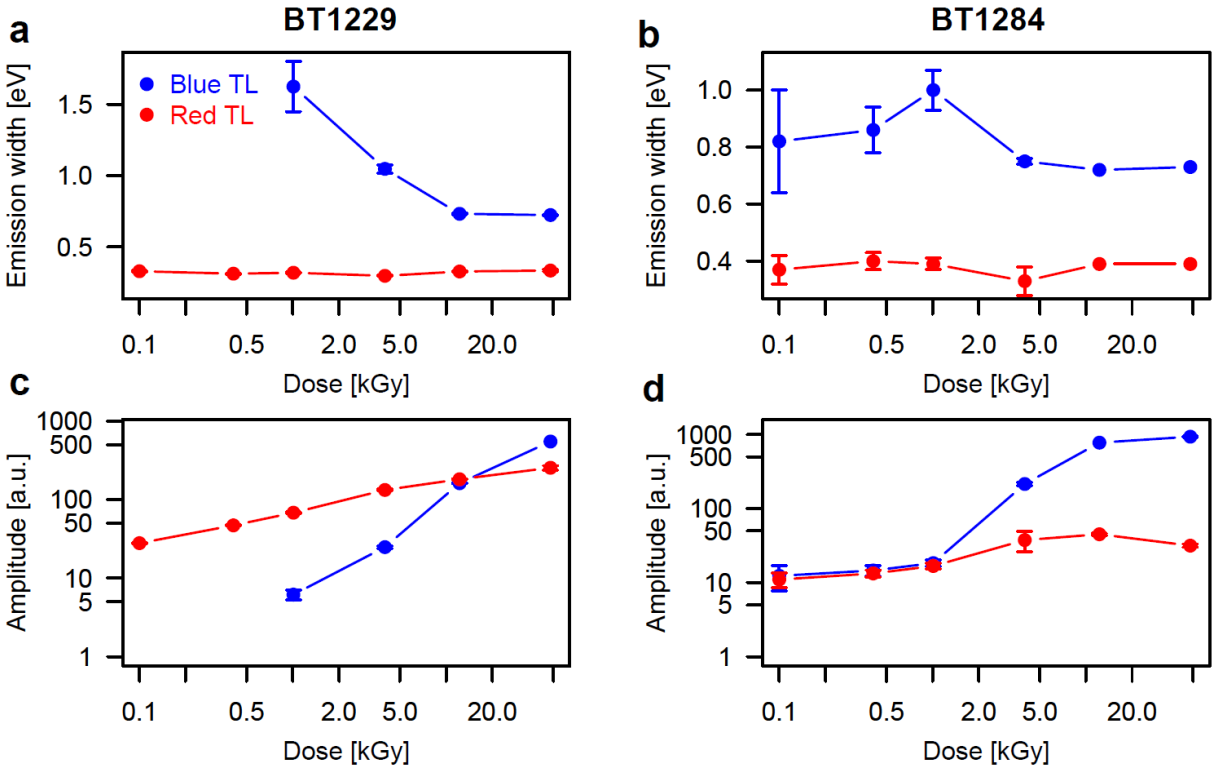


**Fig. 5** Parameters of the blue and red TL emissions obtained from the Gaussian fits to integrated TL spectra in the temperature range 260–300 °C as a function of dose in the range 0.1–47.9 kGy for samples BT1229 and BT1284. The blue emission of sample BT1229 for doses <1 kGy was too dim for evaluation. Subplots show the emission width of the red and blue TL emissions (full width at half maximum, FWHM; a,b) and their amplitude (c,d).

Due to the deviation of the BTL and RTL dose response (as derived from Gaussian curve fitting) from an exponentially saturating function, the characteristic onset of dose saturation ($D_0$) could not be determined. BTL and RTL emissions of sample BT1229 continue to grow up to the highest administered γ-dose of 47.9 kGy, although the growth-rate starts to flatten out for doses >12.2 kGy. In contrast, both TL emissions almost stagnate or even decrease (RTL) for doses in excess of 12.2 kGy in case of sample BT1284. The apparent dose saturation (or at least the decrease in growth-rate) of the blue emission of sample BT1284 between 12.2 and 47.9 kGy may be related to the fact that the integrated spectra in the

interval 260–300 °C accounts mostly for the tail of the ~325 °C TL peak (cf. Fig. 3c,d), which might grow with dose at a different rate than the >350 °C TL peak, which itself does not show any indications of saturation in the TL spectra.

It should be further noted that closer inspection of both the contour plots of the spectral measurements (Figs. 2 and 3; right panel) and the peak fitting analysis in Fig. 4 reveals a slight shift in the maximum emission for the BTL with peak temperature, from 2.61 eV (475 nm) for the 200 °C peak to 2.71 eV (457 nm) for the 340–380 °C region of the higher temperature peak. One can assume that the change in emission maximum is due to the emergence of a second emission, next to the 475 nm emission, at higher temperatures. In this case, the spectra in the 340–380 °C region can be fitted by two components with the central emission of the first one being fixed to 475 nm (value of the 200 °C TL peak), yielding a slightly better fit. The second emission is then found to be at 2.89 eV (~430 nm). These values are close to the central wavelengths of the two components of the blue emission identified in RF spectra of natural and synthetic quartz (Martini et al. 2012), which are 440 nm and 480 nm. However, it should be kept in mind that the use of a second component in the fit will always increase the quality of the fit due to the introduction of additional degrees of freedom. Thus, while the hypothesis of two components in the blue emission is compatible with the experimental data, the TL spectrum alone does not prove their existence.

*Monochromatic TL measurements following γ-irradiation*

For additive γ-doses of 0.1 and 0.4 kGy, the spectrally resolved TL signals of samples BT1229 and BT1284 were very low or even below detection level. We therefore measured the monochromatic TL in the blue and red detection window to examine the dose response of these signals in the low γ-dose range and to assess the interference of the BTL signal with the RTL signal and the sensitisation induced by high-dose irradiation followed by the heat treatment of the first TL readout. Fig. 6 shows BTL and RTL glow curves following additive γ-irradiation between 0.1 kGy and 47.9 kGy; the BTL and RTL response to a constant β-test dose after readout of the signals shown in Fig. 6 is depicted in Fig. 7.

In the additive γ-dose range up to 1 kGy, there is just a minor increase in BTL for temperatures >250 °C for BT1284. The non-monotonous dose-response of sample BT1229 in this dose range might be related to inter-aliquot scatter (Fig. 6). For the highest γ-dose of 47.9 kGy, it is remarkable that for sample BT1284 the high-temperature peak shifts from ~280 °C to ~310 °C in the bulk glow curve, leaving an asymmetric peak with a shoulder towards lower temperatures (Fig. 6c). This pattern can also be recognised in the TL spectra of this sample (Fig. 3). A common feature for samples BT1229 and BT1284 is the increase of the 180 °C BTL and RTL peaks with additive doses up to 12.2 kGy, while they drop again in intensity for even larger doses. In contrast, the BTL and RTL signals recorded at temperatures >250 °C keep on growing over the entire γ-dose range. Such behaviour of dose-dependent change of proportions between low- and high-temperature glow peaks was also observed in the TL spectra of these samples.

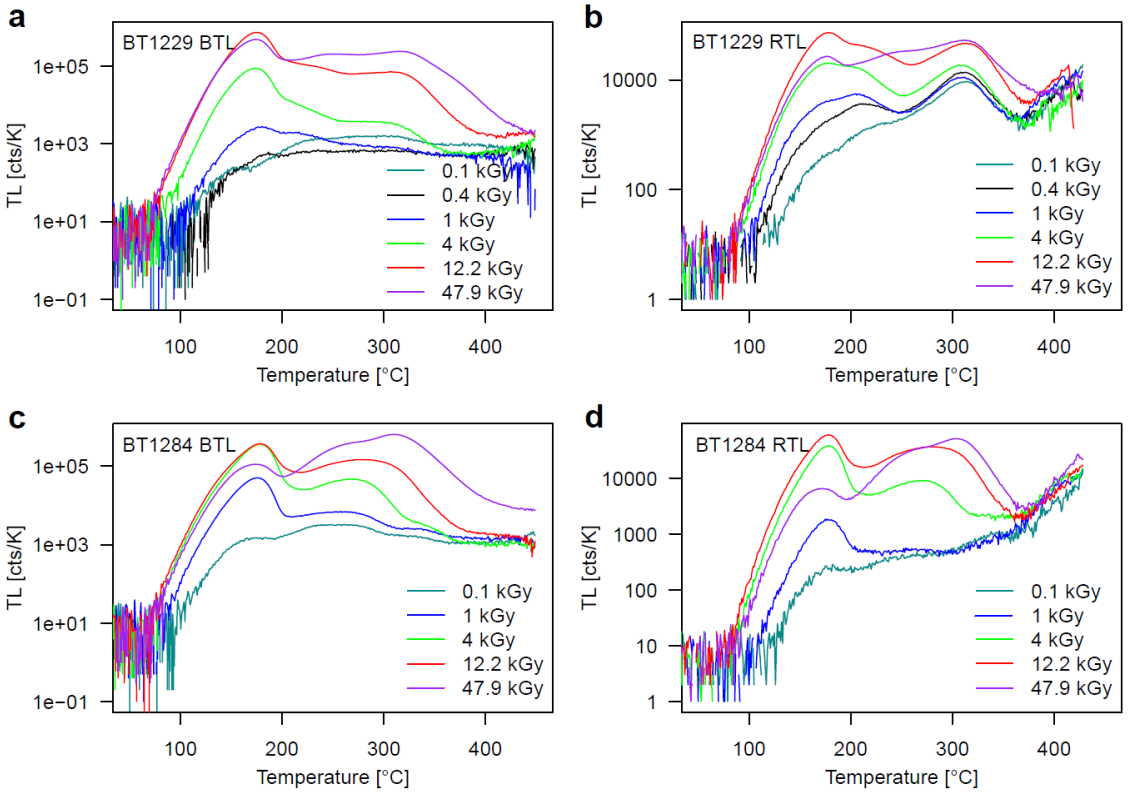


300

**Fig. 6** Monochromatic blue TL (BTL) and red TL (RTL) glow curves of samples BT1229 (a,b) and BT1284 (c,d) following additive γ-irradiation (NTL+ γ) with the doses indicated in the legend.

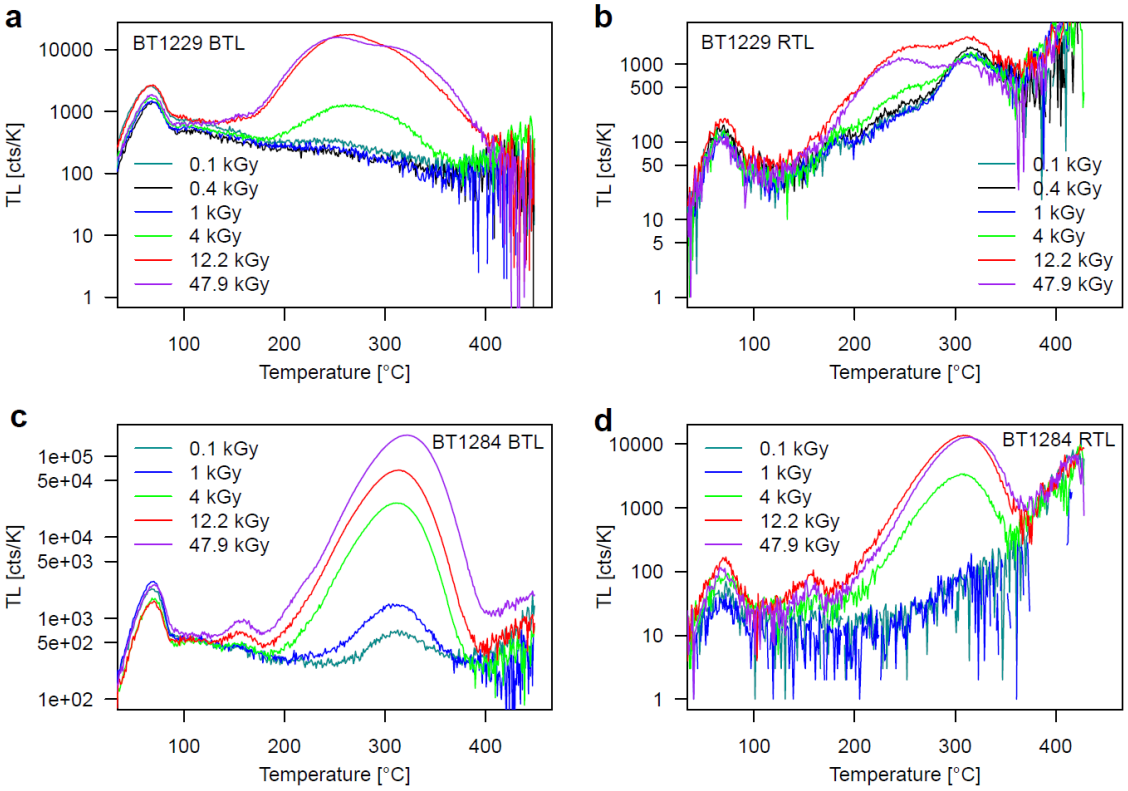


305

**Fig. 7** Monochromatic blue TL (BTL) and red TL (RTL) glow curves of samples BT1229 (a,b) and BT1284 (c,d), recorded after TL readout of the γ-irradiated samples (see Fig. 6) and administering a β-test dose of 50 Gy. The γ-pre-dose is shown in the legend.

As is evident from the TL curves of the second-glow measurements following a 50 Gy β-test dose, the BTL sensitivity of the samples is pre-dose dependent (Fig. 7), so that the NTL+γ signals cannot be normalised using the second-glow signals. BTL dose sensitivity is considerably enhanced by factors of ~50 (BT1229) and ~200 (BT1284) after administering additive γ-doses ≥4 kGy (Fig. 7). The same seems to apply to the RTL signal of sample BT1284 (factor ~120), whereas for BT1229 no systematic change of the RTL sensitivity with dose can be seen; the randomness of the signal intensity for the different doses is more likely linked to inter-aliquot variation.

*Radiofluorescence spectra following additive γ-irradiation*

In contrast to TL emission spectra, the UV is the dominant emission in RF spectra for samples BT1229 and BT1284 and more intense than the blue emission, as shown in Fig. 8. The difference in the relative intensities of the UV emission in RF and TL is a consequence of the strong thermal quenching of this emission at higher temperatures (Schilles et al. 2001). Apart from this, the RF emissions show a more complex evolution with dose and are less straightforward to interpret than the TL spectra. For sample BT1229 a strong decrease in the originally pronounced red emission is evident, with a comparatively small decrease in the UV and almost none in the blue wavelength region. For sample BT1284, on the other hand, an increase in the blue emission (and to a lesser extent also in the UV emission) with dose is seen, whereas no signal change is observed in the wavelength region of the red emission.

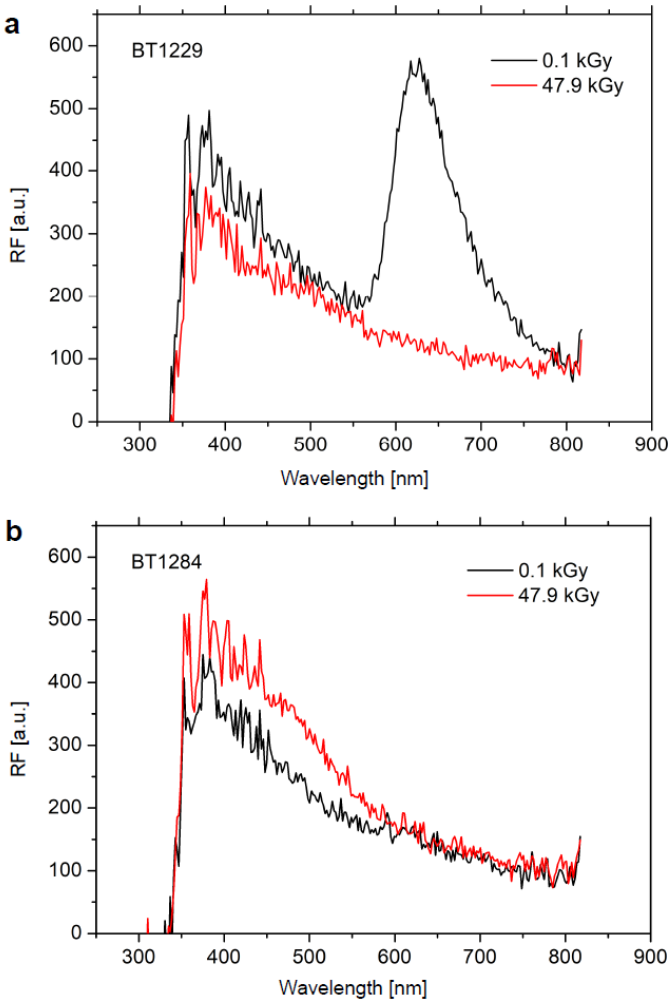


**Fig. 8** Radiofluorescence spectra of sample BT1229 (a) and BT1284 (b), recorded after imparting additive γ-doses of 0.1 and 47.9 kGy. See the main text for details on the measurement configuration.

*Monochromatic TL measurements following β-irradiation*

To explore the dose response of the BTL and RTL emissions for samples from different origin with natural doses >1 kGy, additive β-doses of 2.2 kGy were administered to samples BT1385, BT1629 and BT1647 before measuring their BTL and RTL signals. In this experiment, sample BT1647 served as a reference sample since it derives from the same lithological unit as sample BT1284. Inter-aliquot reproducibility of BTL in the range 250–350 °C was better than 10% ($n$ = 3; except for BT1385: 30%) and no normalisation was applied.

Natural (NTL) glow curves and those resulting from additive β-irradiation (NTL+β) show that for two of the three samples (BT1385, BT1647) the TL signal above 250 °C continues to increase with an additive β-dose of 2.2 kGy (Fig. 9). Because electron traps giving rise to TL >250 °C are generally considered as deep enough not to drain electrons over geological timescales, this observation implies that the BTL signal has not yet reached its dose saturation level in this region of the TL glow curve. However, the NTL+β signal does not further increase compared to NTL for sample BT1629 that carries a natural dose in the order of a few hundred kGy. Reasons for this observation could be that either the increase in BTL response to the 2.2 kGy additive dose is too small to be resolved (given the 10% inter-aliquot scatter), or the BTL signal is in dose saturation in the glow curve region 250–450 °C. The BTL glow curve in the temperature range <250 °C shows an intense peak at ~180 °C (BT1385, BT1647), which most likely corresponds to the BTL emission at 200 °C observed in the TL spectra of samples BT1229 and BT1284 (see Figs. 2 and 3). Further low-temperature BTL peaks appearing at ~80 °C and ~105 °C are probably the well-known '110 °C' and '160 °C' TL peaks in quartz, that are observed at the latter temperatures for higher heating rates than used in this study (Aitken 1985; Spooner and Questiaux 2000; Veronese et al. 2004).

For glow curve temperatures >250 °C, a similar picture emerges for the RTL emission of these three samples, i.e., the NTL+β glow curves exceed the NTL glow curves in case of BT1385 and BT1647, while the RTL signal of BT1629 is of the same intensity for both NTL and NTL+β. Similarly, low temperature RTL peaks occur at the same positions, except for a peak at around 150 °C, which surpasses the 200 °C signal of sample BT1647. BTL and RTL glow curves recorded for BT1647 are in qualitative agreement with the TL spectra of sample BT1284, while TL peaks are shifted ~20 °C towards lower temperatures compared to the spectra.

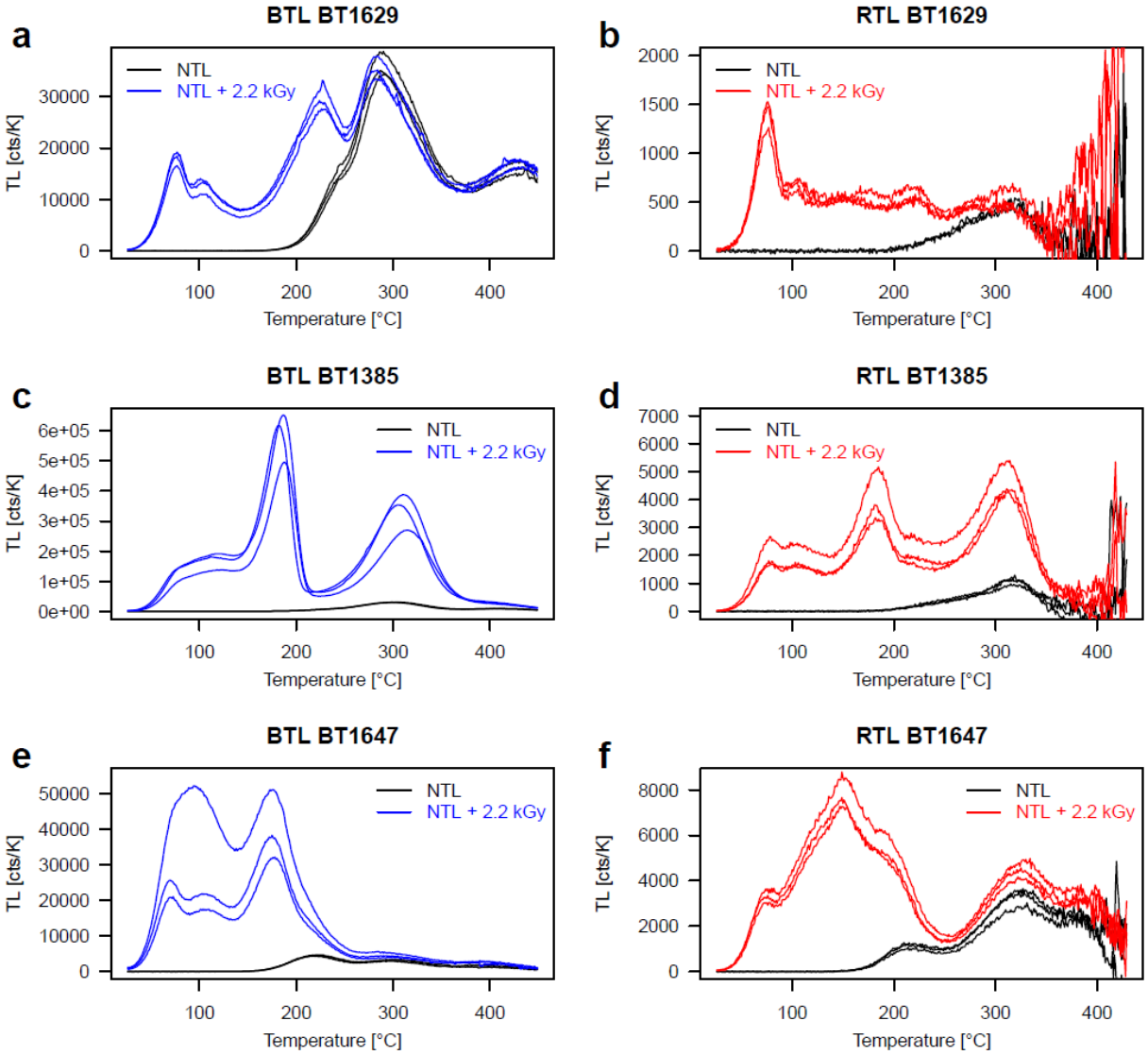


**Fig. 9** Monochromatic blue TL (BTL) and red TL (RTL) glow curves of samples BT1629 (a,b), BT1385 (c,d) and BT1647 (e,f) following an additive β-dose of 2.2 kGy (NTL+β). Three aliquots were measured for both NTL and NTL+β; no normalisation was performed. All samples carry (expected) natural doses in excess of 1 kGy. For more details on sample characteristics and measurement parameters, see the main text.

## Discussion

*Interpretation of RF spectra and second glow RTL signals*

Complex behaviour of the RF emissions in quartz with dose has also been observed by other authors, with dose-response varying from increase, decrease to "peak shaped" (first increase, then decrease) with dose, for all three emissions (Krbetschek and Trautmann 2000; Woda et al. 2002; Shimizu et al. 2006; Martini et al. 2012; Friedrich et al. 2017). Generally, RF is a result of the simultaneous hole trapping and electron recombination at the recombination centre, which is to a first approximation proportional to the excitation rate and thus to the dose-rate (Friedrich et al. 2018). In how far and how this recombination rate changes with dose depends on the relative concentrations of defects in the crystal and their degree of interaction during irradiation. Despite this complexity, it is reasonable to assume that for low doses (beginning of irradiation), with the number of trapped charges being much smaller than the number of available trapping sites, the relative RF intensity, for samples with similar properties, will be dependent on the respective concentration of defects (trapping sites). Thus, the strong red RF emission in sample BT1229 is an indication of a higher concentration of defects responsible for this

emission than in sample BT1284, and this is also reflected in the TL spectra (compare 1 kGy spectra for BT1284 and BT1229; Figs. 2–4).

Considering the apparent discrepancy in the behaviour of the second glow RTL signals between samples BT1229 and BT1284 (Fig. 7), this can be resolved by considering that the RTL signal of sample BT1284 is likely to be strongly influenced, if not entirely dominated, by the blue emission in a PMT measurement (Fig. 4). Thus, the apparent sensitivity enhancement of the RTL signal by a factor of ~120 is most likely a simple copy of the sensitivity enhancement of the BTL signal. In light of this, the results for the RTL signal of both samples are compatible with the absence of any pre-dose dependence for this signal, which is in accordance with previous studies (Huntley et al. 1988a,b).

*Emission spectra and quartz formation*

Despite the large saturation doses often associated with the RTL emission of quartz (Fattahi and Stokes 2000, 2003), it has been reported for epithermal vein quartz and pegmatitic quartz samples that the RTL signal approaches saturation for doses >1 kGy, while the BTL emission continues to grow for doses in excess of 10 kGy (Hashimoto et al. 1987). Specifically, the BTL emission surpasses the RTL emission in intensity at a dose of about 1 kGy in the pegmatitic quartz investigated by Hashimoto et al. (1987). This 'transitional' dose indicative for the shift from predominantly red to blue luminescence is in the same order of magnitude as observed for samples BT1229 and BT1284 in this study and for the fired quartz examined by Woda et al. (2002). Particularly, Hashimoto et al. (1987) attribute this feature to the 'intermediate' hypabyssal nature of this type of quartz in between the end members of volcanic quartz and plutonic quartz, emitting either primarily in the red or the blue range, respectively, over the entire investigated dose range. These observations, that were obtained as monochromatic TL glow curves using optical filters, are in line with our spectral data derived from plutonic (granitic) quartz (BT1229, BT1284). Similarly, also other samples (BT1385, BT1647) examined in this study showed a disproportionately intense growth of the blue TL emission following a 2.2 kGy additive β-dose, especially in the temperature region around 180 °C. Since the majority of sedimentary quartz grains derives from plutonic quartz, this characteristic TL behaviour in the high-dose range might not be restricted to hypabyssal types of quartz, but represent a more widespread feature.

*Emission spectra and associated defects*

Similar results compared to our findings were obtained by Chawla et al. (1998) who compared the TL sensitivity change in quartz samples carrying identical large doses, but imparted once at natural dose rate (~2 Gy $ka^{-1}$) and once at laboratory dose rate (~0.05 Gy $s^{-1}$). They report on a substantial increase of BTL sensitivity for laboratory γ-doses >250 Gy, and on a pronounced pre-dose effect as also observed by Huntley et al. (1988a) and Woda et al. (2002). The blue band in quartz (~2.65 eV) is usually ascribed to recombination at (paramagnetic) $[AlO_4]^0$ sites (e.g., McKeever 1991; Rendell et al. 1994; Woda et al. 2002, Guzzo et al. 2017). This centre is created from the diamagnetic precursor $[AlO_4/M^+]^0$ by hole capture, where $M^+$ is a charge compensating ion ($Li^+$, $Na^+$ or $H^+$) attached to the initial $Al^{3+}$ site. After hole capture, the alkali or hydrogen ion is no longer necessary for charge compensation and can diffuse through the open c-axis channels of the crystal until attached to an electron trap $[DO_4]^-$, where D stands for, e.g., Ge, Ti or other unknown defects. In this way the stable electron centre $[DO_4/M^+]^0$ is formed (Weil 1984). Guzzo et al. (2017) propose that the $[GeO_4/Li^+]^0$ centre acts as the electron trap for the intermediate TL peak, which in their samples occurred at 240 °C, while the $E_1$' centre (oxygen vacancy filled with one electron) is the electron trap for the ~325 °C TL peak. In contrast, Schilles et al. (2001) assign the $E_1$' centre to a competing recombination centre, where recombinations occur either non-radiative or outside the detection window. Chawla et al. (1998) suggest that the alkali ion itself can form the electron trap, after localisation at an interstitial position. This would essentially correspond to an $[SiO_4/M^+]^0$ centre, which has been shown to be unstable at room temperature and responsible for the TL peak at 190 K (-83 °C), so its involvement in the formation of TL peaks above room temperature is rather unlikely (Martini et al. 2000).

The attribution of γ-induced BTL to the $[AlO_4]^0$ centre was also proposed by Plötze et al. (2012) based on EPR measurements and TL spectrometry, which demonstrated an EPR saturation dose of this centre of ~1 MGy. The fact that no increase in the BTL >250 °C could be induced by additive β-irradiation of sample BT1629 (estimated natural dose of a few hundred kGy) while younger samples still yielded growing BTL signals in that temperature region supports the assignment of the $[AlO_4]^0$ centre to this emission and indicates that this centre is stable over geological periods. This is also corroborated by recent results in Hunter et al. (2018), who have estimated a lifetime of the 350 °C BTL peak in quartz after 4 kGy β-dose of 6.2 Ma at 20 °C.

The abrupt increase of BTL sensitivity at a threshold dose of ~1 kGy (Figs. 2–4) could in principle be explained by the creation of new traps, the removal of competing, non-radiative pathways or a combination of both. Chawla et al. (1998) observe a new EPR centre of unknown nature, that is created by irradiation and subsequent heating to 500 °C which the authors link to the sensitivity increase of the BTL, but to date the existence of this centre has not been confirmed in independent studies. Guzzo et al. (2017) suggest that the removal of a non-radiative recombination pathway within the Al-centre, which the authors link to the thermal quenching mechanism in quartz (Pagonis et al. 2011, 2014) and which is induced by high-dose irradiation and subsequent heat treatment (400 °C), could result in an enhanced radiative recombination rate at higher doses. Woda et al. (2002) speculate that the enhanced generation of BTL beyond laboratory doses of 1 kGy might be related to the decay of the $[GeO_4/Li^+]^0$ centre and the associated redistribution of released Li ions above this threshold dose. Common to the different suggested mechanisms is that the dose-induced sensitivity enhancement of BTL in the temperature range 250–380 °C occurs during the TL readout (heating) stage and not during the irradiation stage, so that the number of blue-emitting recombination centres before readout is expected to grow continuously with dose. This is in agreement with the reported dose-response of the Al centre (Woda et al. 2002) and the absence of any strong increase of the blue emission in the RF spectra of both samples for the highest dose (Fig. 8).

Furthermore, the almost constant value of the Al signal intensity after a TL measurement independent of dose, as shown in Woda et al. (2002), make it unlikely that the pre-dose information is connected to changes in the population of the recombination centre but rather can be found in processes involving the electron trap(s). It might be worthwhile considering whether this pre-dose effect can be used to estimate an accumulated dose and thus for dating purposes.

The decrease of the 200 °C BTL peak at higher doses (Fig. 6) could potentially be explained by a double electron capture at the electron trap, with the two types of traps (occupied with one or two electrons) having different activation energies. Such an approach has been used to simulate the non-monotonous dose-response of the Ge- and Ti-centres in quartz (Woda and Wagner 2007) and has recently been further developed for TL (Chen et al. 2017). It would be in line with the suggested assignment of the electron trap for this TL peak to the $[GeO_4/Li^+]^0$ centre by Guzzo et al. (2017). An alternative explanation would be competition effects between the blue and a non-radiative recombination centre during heating (TL readout), with the latter growing much more rapidly with dose than the former, leading to a decrease in the amount of radiative recombination at higher doses (Lawless et al. 2005). A sharp drop in signal intensity for the 210 °C BTL signal has also been observed by Hunter et al. (2018) for doses higher than 16 kGy, however, for their samples the higher temperature BTL peak (350 °C) also dropped in a similar fashion in this dose range, which is not the case for the samples studied here.

For the red emission in quartz there is no clear link to a specific type of defect (Krbetschek et al. 1997). However, in contrast to King et al. (2011) who detected an increase of RTL at the expense of BTL following high-dose (>100 MGy) proton irradiation, we did not observe a trade-off between blue and red TL emissions in our samples for the γ-dose range investigated. Neither the amplitude of the blue nor that of the red spectral component decreases with dose in the TL region >250 °C.

*Implications for TL dating and thermochronometry*

The TL spectra acquired in this study explain the 'uncommon' shape of additive-dose RTL glow curves constructed for the plutonic quartz samples from the geothermal drill hole, as presented in Schmidt et al. (2015). Especially for sample BT1284, it is the strong BTL emission that masks the red emission for doses in the kGy range. An overlap of the RTL signal with another emission reaching into the red detection window could provide an explanation for similar observations of RTL glow curves made for higher laboratory doses (e.g., Montret et al. 1992; Fattahi and Stokes 2000).

Thus, when detecting monochromatic TL glow curves in the red window (usually centred on ~620 nm), the recorded signal may contain contributions from both the red-emitting centre and the tail of the blue emission that might in intensity exceed the red signal. The degree of interference is a result of the relative intensities of the blue and red emission and seems to be sample-dependent. As shown for sample BT1229, in some circumstances a signal dominated by the red emission might still be detected. Given the observed width of the blue emission at high doses, it does not appear to be possible to separate the blue and red bands by means of optical filters alone. The only way of deconvolving the two emissions and of being able to judge the reliability of a monochromatic measurement is to conduct spectrometric measurements. Although more experiments are definitely needed, TL results for sample BT1629 indicate the long-term stability of the BTL emission at glow temperatures >250 °C. Consequently, palaeodose estimates derived from a mixed blue-red TL emission might be reliable if the common quality assurance criteria are met (e.g., $D_e$ plateau test). However, before such dose measurements can be deemed trustworthy, rigorous further investigations are necessary.

## Conclusion

Our new TL spectral data obtained for two igneous quartz samples in the γ-dose range 0.1–47.9 kGy show that the spectra are mainly composed of two emissions at 2.67 eV (~465 nm) and 1.95 eV (630 nm). The blue emission, that shows a pre-dose effect, increases in intensity with dose and completely dominates the spectrum for doses >12 kGy for one sample. Whereas paramagnetic $[AlO_4]^0$ sites are the likely origin of the blue emission, its sharp increase in sensitivity above ~1 kGy might be related to the creation of new traps, the dose-induced redistribution of alkali ions and/or the removal of non-radiative competitive recombination pathways. Supplementing radiofluorescence spectra support the hypothesis that the blue TL sensitivity change is linked to the electron traps rather than to the recombination centres. Furthermore, monochromatic TL measurements (blue and red detection window) of quartz samples in natural dose saturation indicate that the blue emission is thermally stable enough to be used for geological dating and dosimetry. Finally, the dominance of the blue spectral component well explains the unexpected shape of red TL glow curves in the kGy range in previous studies. The relative brightness of blue and red TL at high doses, however, seems to be sample dependent and difficult to predict, so that spectral measurements in combination with monochromatic TL analyses are advised when aiming for the red component. More investigations are certainly needed to fully explore the nature and luminescence properties especially of the blue TL emission at high doses.

## Acknowledgements

We acknowledge support of the Oberfrankenstiftung (Projekt “Niedrigst-Temperatur-Thermochronometrie mittels Thermolumineszenz (Thermalbohrung Weißenstadt)”) and thank Johannes Friedrich for technical assistance. Part of this work was supported by a postdoc fellowship of the German Academic Exchange Service (DAAD, ID 57360695). We thank the two anonymous reviewers for their helpful comments.

**References**


Aitken M (1985) Thermoluminescence dating. Academic Press, London

Ames CJ, Nowell A, Cordova CE, Pokines JT, Bisson MS (2014) Paleoenvironmental change and settlement dynamics in the Druze Marsh: Results of recent excavation at an open-air Paleolithic site. Quaternary International 33:60-73

Ames CJH, Cordova CE (2015) Middle and Late Pleistocene Landscape Evolution at the Druze Marsh Site in Northeast Jordan: Implications for Population Continuity and Hominin Dispersal. Geoarchaeology 30:307-329

Briceño HO, Schubert C (1990) Geomorphology of the Gran Sabana, Guyana Shield, Southeastern Venezuela. Geomorphology 3:125-141

Briceño HO, Schubert C, Paolini J (1990) Table-mountain geology and surficial geochemistry: Chimanta Massif Venezuelan Guyana Shield. J S Amer Earth Sci 3:179-194

Chalcraft D, Pye K (1984) Humid tropical weathering of quartzite in southeastern Venezuela. Z Geomorph NF 28:321-332

Chawla S, Rao TG, Singhvi AK (1998) Quartz thermoluminescence: dose and dose-rate effects and their implications. Radiat Meas 29:53-63

Chen R, Lawless JL, Pagonis V (2017) Thermoluminescence associated with two-electron traps. Radiat Meas 99:10-17

Doerr SH (1999) Karst-like landforms and hydrology in quartzites of the Venezuelan Guyana shield: Pseudokarst or real karst? Z Geomorph NF 43:1-17

Fattahi M, Stokes S (2000) Extending the time range of luminescence dating using red TL (RTL) from volcanic quartz. Radiat Meas 32:479-485

Fattahi M, Stokes S (2003) Dating volcanic and related sediments by luminescence methods: a review. Earth Sci Rev 62:229-264

Friedrich J, Fasoli M, Kreutzer S, Schmidt C (2017) The basic principles of quartz radiofluorescence dynamics in the UV – analytical, numerical and experimental results. J Lumin 192:940-948

Friedrich J, Fasoli M, Kreutzer S, Schmidt C (2018) On the dose rate dependence of radiofluorescence signals of natural quartz. Radiat Meas 111:19-26

Ganzawa Y, Maeda M (2009) 390–410 °C isothermal red thermoluminescence (IRTL) dating of volcanic quartz using the SAR method. Radiat Meas 44:517-522

Guzzo PL, de Souza LBF, Barros VM, Khoury HJ (2017) Spectroscopic account of the point defects related to the sensitization of TL peaks beyond 220 °C in natural quartz. J Lumin 188:118-128

Hashimoto T, Yokosaka K, Habuki H (1987) Emission properties of thermoluminescence from natural quartz-blue and red TL response to absorbed dose. Nucl Tracks Rad Meas 13:57-66

Hashimoto T, Kojima M, Shirai N, Ichino M (1993) Activation energies from blue- and red-thermoluminescence (TL) of quartz grains and mean lives of trapped electrons related to natural red-TL. Nucl Tracks Rad Meas 21:217-223

Hunter PG, Spooner NA, Smith BW (2018) Thermoluminescence emission from quartz at 480 nm as a high-dose radiation marker. Radiat Meas 120:143-147

Huntley DJ, Godfrey-Smith DI, Thewalt MLW, Berger GW (1988a) Thermoluminescence spectra of some mineral samples relevant to thermoluminescence dating. J Lumin 39:123-136

Huntley DJ, Godfrey-Smith DI, Thewalt MLW, Prescott JR, Hutton JT (1988b) Some quartz thermoluminescence spectra relevant to thermoluminescence dating. Nucl Tracks Radiat Meas 14:27-33

Itoh N, Stoneham D, Stoneham A (2002) Ionic and electronic processes in quartz: mechanisms of thermoluminescence and optically stimulated luminescence. J Appl Phys 92:5036-5044

Jain M, Duller GAT, Wintle A (2007) Dose response, thermal stability and optical bleaching of the 310 °C isothermal TL signal in quartz. Radiat Meas 42, 1285-1293

King GE, Finch A, Robinson R, Hole D (2011) The problem of dating quartz 1: Spectroscopic ionoluminescence of dose dependence. Radiat Meas 46:1-9

King GE, Guralnik B, Valla PG, Herman F (2016a) Trapped-charge thermochronometry and thermometry: A status review. Chem Geol 446:3-17

King GE, Herman F, Lambert R, Valla P, Guralnik B (2016b) Multi-OSL-thermochronometry of feldspar. Quat Geochronol 33:76-87

Kolb T, Fuchs M, Zöller L (2016) Deciphering fluvial landscape evolution by luminescence dating of river terrace formation: a case study from Northern Bavaria, Germany. Z Geomorph 60:29-48

Krbetschek MR, Götze J, Dietrich A, Trautmann T (1997) Spectral information from minerals relevant for luminescence dating. Radiat Meas 27:695-748.

Krbetschek MR, Trautmann T (2000) A spectral radioluminescence study for dating and dosimetry. Radiat Meas 32:853-857

Kuhn R, Trautmann T, Singhvi AK, Krbetschek MR, Wagner GA, Stolz W (2000) A study of thermoluminescence emission spectra and optical stimulation spectra of quartz from different provenances. Radiat Meas 32:653-657

Lawless JL, Chen R, Lo D, Pagonis V (2005) A model for non-monotonic dose dependence of thermoluminescence (TL). J. Phys. Condens. Matter 17:737-753

Martini M, Meinhardi F, Vedda A (2000) The role of alkali ions in the 190 K TSL peak in quartz. Radiat Meas 32:673-677

Martini M, Fasoli M, Villa I, Guibert P (2012) Radioluminescence of synthetic and natural quartz. Radiat Meas 47:846-850

McKeever SWS (1991) Mechanisms of thermoluminescence production: Some problems and a few answers? Nucl Tracks Rad Meas 18:5-12

Miallier D, Faïn J, Sanzelle S, Pilleyre T, Montret M, Soumana S, Falgères C (1994) Attempts at dating pumice deposits around 580 ka by use of red TL and ESR of xenolithic quartz inclusions. Radiat Meas 23:399-404

Montret M, Miallier D, Sanzelle S, Fain J, Pilleyre T, Soumana S (1992) TL dating in the Holocene using red TL from quartz. Ancient TL 10:33-36

Murray AS, Wintle AG (2000) Application of the single-aliquot regenerative-dose protocol to the 375°C quartz TL signal. Radiat Meas 32:579-583

Pagonis V, Lawless J, Chen R, Chithambo ML (2011) Analytical expressions for time-resolved optically stimulated luminescence experiments in quartz. J Lumin 131:1827-1835

Pagonis V, Chithambo ML, Chen R, Chruścińska A, Fasoli M, Li SH, Martini M, Ramseyer K (2014) Thermal dependence of luminescence lifetimes and radioluminescence in quartz. J Lumin 145:38-48

Pilleyre T, Montret M, Faïn J, Miallier D, Sanzelle S (1992) Attempts at dating ancient volcanoes using the red TL of quartz. Quat Sci Rev 11:13-17

Plötze M, Wolf D, Krbetschek MR (2012) Gamma-Irradiation Dependency of EPR and TL-Spectra of Quartz. In: Götze J, Möckel R (eds) Quartz: Deposits, Mineralogy and Analytics. Springer, Heidelberg, pp 177-190.

Reiners PW, Brandon MT (2006) Using Thermochronology to Understand Orogenic Erosion. Annu Rev Earth Pl Sc 34:419-466

Rendell HM, Townsend PD, Wood RA, Luff BJ (1994) Thermal treatments and emission spectra of TL from quartz. Radiat Meas 23:441-449

Richter D, Krbetschek M (2006) A new thermoluminescence dating technique for heated flint. Archaeometry 48:695-705

Richter D, Pintaske R, Dornich K, Krbetschek M (2012) A novel beta source design for uniform irradiation in dosimetric applications. Ancient TL 30:57-63

Richter D, Richter A, Dornich K (2013) Lexsyg - A new system for luminescence research. Geochronometria 40:220-228

Richter D, Klinger P, Schmidt C, van den Bogaard P, Zöller L (2017) New chronometric age estimates for the context of the Neanderthal from Wannen-Ochtendung (Germany) by TL and argon dating. Journal of Archaeological Science: Reports 14:127-136

Rink WJ, Rendell H, Marseglia EA, Luff BJ, Townsend PD (1993) Thermoluminescence spectra of igneous quartz and hydrothermal vein quartz.
Phys Chem Min 20:353-361

Schilles T, Poolton N, Bulur E, Bøtter-Jensen L, Murray AS, Smith G, Riedi P, Wagner GA (2001) A multi-spectroscopic study of luminescence sensitivity changes in natural quartz induced by high-temperature annealing. J Phys D Appl Phys 34:722-731

Schmidt C, Friedrich J, Zöller L (2015) Thermochronometry using red TL of quartz? - Numerical simulation and observations from in-situ drill-hole samples. Radiat Meas 81:98-103

Scholefield RB, Prescott JR (1999) The red thermoluminescence of quartz: 3-D spectral measurements. Radiat Meas 30:83-95

Scholefield RB, Prescott JR, Franklin A, Fox P (1994) Observations on some thermoluminescence emission centres in geological quartz. Radiat Meas 23:409-412

Shimizu N, Mitamura N, Takeuchi A, Hashimoto T (2006) Dependence of radioluminescence on TL-properties in natural quartz. Radiat Meas 41:831-835

Spooner NA, Questiaux DG (2000) Kinetics of red, blue and UV thermoluminescence and optically-stimulated luminescence from quartz. Radiation Measurements 32:659-666

Townsend PD (1994) Analysis of TL emission spectra. Radiat Meas 23:341-348

Veronese I, Giussani A, Göksu H, Martini M (2004) The trap parameters of electrons in intermediate energy levels in quartz. Radiation Measurements 38:743-746

Weil JA (1984) A review of electron spin spectroscopy and its application to the study of paramagnetic defects in crystalline quartz. Phys Chem Minerals 10:149-165

Westaway K, Prescott J (2012) Investigating signal evolution: A comparison of red and UV/blue TL, and UV OSL emissions from the same quartz sample. Radiat Meas 47:909-915

Wintle AG (2008) Fifty years of luminescence dating. Archaeometry 50:276-312

Woda C, Schilles T, Rieser U, Mangini A, Wagner GA (2002) Point defects and the blue emission in fired quartz at high doses: a comparative luminescence and EPR study. Radiat Prot Dosim 100:261-264

Woda C, Wagner GA (2007) Non-monotonic dose dependence of the Ge- and Ti-centres in quartz. Radiat Meas 42:1441-1452

Zöller L, Richter D, Blanchard H, Einwögerer T, Händel M, Neugebauer-Maresch C (2014) Our oldest children: Age constraints for the Krems-Wachtberg site obtained from various thermoluminescence dating approaches. Quaternary International 351:83-87